UNIVERSITY OF
BATH

Link to publication

University of Bath

Observation and Analysis of Phase-Locking in Parabolic Bow-Tie Laser Arrays

F. Causa, *Member, IEEE*, and D. Masanotti

Abstract—This paper presents experimental and theoretical results to show that in-phase coherent coupling occurs in high-power arrays of parabolic bow-tie lasers. Such devices require simple and inexpensive device fabrication, thus providing a cost-effective high-power laser for high-brightness operation at 980 nm. The maximum brightness achieved was 318 MW·cm^{-2}sr^{-1} at 20 times the threshold with far-field full-width at half-maximum less than 1.5 times the diffraction limit, measured without the use of external lenses under low-duty cycle (0.1%) pulsed operation. Results obtained from double-slit interference experiments show a clear distinction between phase-coherent arrays and corresponding arrays of independent emitters.

Index Terms—High-brightness, high-power, index-guiding, laser arrays, phase-locking, tapered geometry.

I. INTRODUCTION

WITH the widespread use of laser diodes in many different sectors of modern industry there has been an increasing demand for high optical output power devices with good beam quality and, ideally, low production and packaging costs. High optical output power can in principle be achieved by increasing the active volume, either by using broad-area lasers or by operating several lasers in arrays or bars. However, it has been recognized that to achieve the highest brightness from an array of laser diodes it is necessary to achieve parallel coupling, where all devices are coupled to one another in the same measure, and excite only the fundamental array mode ("in-phase coupling"), [1]. In-phase coupling is difficult to achieve in a simple array of narrow stripe lasers because the modal gain of the highest order array mode is higher than that of the fundamental mode, e.g., [2], resulting in an undesirable two-lobed far-field intensity pattern, characteristic of the "out-of-phase" coupling. Fundamental array mode operation and, therefore, high brightness have been achieved with resonant optical waveguide laser arrays, [3]. However, this device design requires demanding material growth and device fabrication, i.e., high costs. On the other hand, phase-locked arrays of parabolic bow-tie lasers (PBTLs) have been designed to achieve high power and high brightness without the need for regrowth or sophisticated device fabrication, [4]. The novelty of the parabolic bow-tie laser arrays (PBTLAs) discussed here is that the inter-element coupling is longitudinally nonuniform because of

the array geometry, thereby promoting stability of operation as discussed in [5] where the optical guiding properties of these novel devices were described in detail. PBTLAs can be seen as a collection of tapered lasers operated simultaneously or as a broad area laser with an integrated spatial filter. In the either case, it is not possible to define an analytic expression for the modes of the structure. Therefore, in the first analysis the CMT (coupled-mode theory), [6], has been used to study the PBTLA as a collection of lasers that are coupled only at the facets.

This paper presents experimental and theoretical results obtained from arrays of parabolic bow-tie laser diodes designed to achieve high power with high brightness with simple and inexpensive device fabrication and packaging, and without the need of external optics. The results discussed here have been obtained predominantly under (low-duty cycle) pulsed conditions, with preliminary CW results. The operation of the arrays presented in this paper is affected by thermal lensing which promotes multi-array-mode operation, [5], unlike the case of (high-)index-antiguided devices which have been demonstrated to produce stable near-diffraction-limited output beam under CW operation, [7]. The devices characteristics are presented in Section II. Experimental and theoretical results for different devices (varying geometry and inter-element separation) are presented in Section III to prove that fundamental array mode operation can be achieved in certain conditions. Experimental results estimating the degree of coherence of PBTLAs without and with inter-element separation are presented and discussed in Section IV. The conclusions drawn from the above discussions are summarized in Section V.

II. DEVICE FABRICATION AND GEOMETRY

The laser arrays discussed in this paper have been fabricated from a double hetero-structure, large-optical-cavity, triple-quantum-well (TQW) semiconductor material specially designed for high power operation at 980 nm [5]. The main material and device parameters estimated from theory or experimental characterization are as follows: (vertical) optical confinement factor in the TQW: $\Gamma = 0.045$; equivalent spot size: $S = (d/\Gamma) = 0.458$ μm where d is the active region thickness; power density before catastrophic optical damage measured under pulsed operation (5-μs pulsewidth): $p_{\text{COD}} = 11$ MW·cm^{-2}; vertical beam divergence [full-width at half-maximum (FWHM)]: $\theta_y = 58°$.

The schematic of a five-element PBTLA (5PBTLA) is presented in Fig. 1. The device geometry is defined by an etched rib which provides an effective index step (estimated to be $\Delta n_{\text{eff}} \sim 0.007$ for etch depth $h_{\text{RIB}} = 0.9$ μm) for weak lateral index-guiding. The etched rib is practical not only to provide weak

The authors are with the Department of Electronic and Electrical Engineering, University of Bath, Bath BA2 7AY, U.K. (e-mail: f.causa@bath.ac.uk; D.Masanotti@bath.ac.uk).
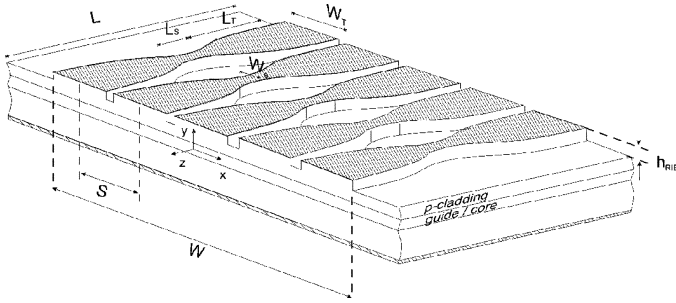
Fig. 1.   Schematic of a five-element PBTLA: W_T is the width of the individual element, W_S is the width of the central straight section, W is the array width; L_T is the taper length, L_S the length of the central straight section and L device length; S the inter-element separation; and h_{RIB} the etch depth.
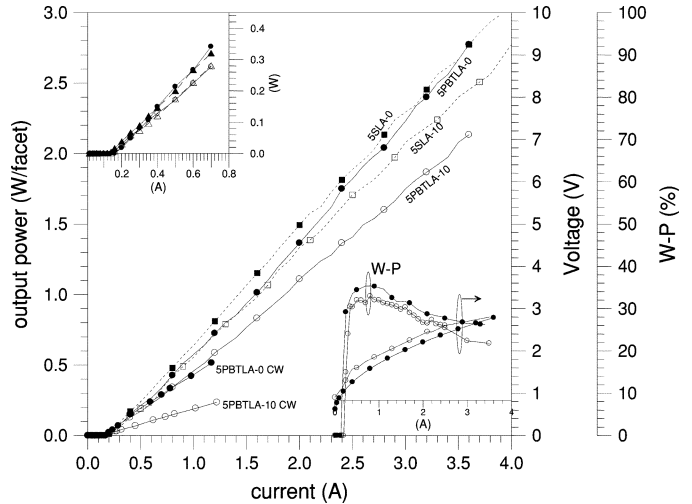

Fig. 2.   Pulsed and CW optical output power per facet as a function of injection current measured from uncoated in-house fabricated 5PBTLA-0s (solid line with full circles), 5SLA-0s (dotted line with full squares), 5PBTLA-10s (solid line with empty circles), and 5SLA-10s (dotted line with empty squares). (Intensity filters have been used to take readings at high power levels.) Representative junction voltage and W-P efficiency (per pulse and per facet) curves are also shown for uncoated 5PBTLA-0 and 5PBTLA-10. Inset: Pulsed optical output power per facet as a function of injection current measured from in-house fabricated 5LBTLA-0s (dashed line with full triangles), 5LBTLA-10s (dashed line with empty triangles), 5PBTLA-0s, and 5PBTLA-10s, as above.

optical guiding, but also to reduce current spreading. The devices have been then modelled using the effective index method to reduce the problem to two dimensions (lateral and longitudinal), and the scalar analysis. To maximize the brightness (both the output power and the lateral beam divergence) the parabolic rib geometry was used, [8], [9], defined by $w(z) = \sqrt{W_S^2 + ((W_T^2 - W_S^2))/(L_T)z}$, where W_S is the rib width at the narrow central section, W_T is the wider width of the taper, and L_T is the taper length (see Fig. 1). For the devices of interest in this paper $W_T = 20 \ \mu m$ and $L_T = 500 \ \mu m$, the width and length of the central straight section are $W_S = 3 \ \mu m$ and $L_S = 50 \ \mu m$. For useful comparisons, corresponding stripe laser arrays (SLAs) for which the width of the individual elements is $W_T =$ constant along the length and linear bow-tie laser arrays (LBTLAs) for which $w(z) = W_S + ((W_T - W_S))/(L_T)z$, were also fabricated. All devices have the same length ($L = 1050 \ \mu m$) and same facet width ($W = 100 \ \mu m$).

Two types of in-house fabricated arrays will be discussed in this paper with different inter-element spacing S, defined as the distance between the longitudinal axes of two adjacent elements (Fig. 1). For the devices presented in this paper, it is either $S = W_T$, in which case the device will be referred to as 5PBTLA-0, or $S > W_T$, in which case the device will be referred to as 5PBTLA-$(S - W_T)$. The inter-element spacing in 5PBTLA-$(S - W_T)$s was chosen to ensure that there was no coupling between elements. To estimate the inter-element spacing required to avoid inter-element coupling, near-field intensity profiles were measured from an individual element at low injection current ($I \ll I_{th}$) with low-pass optical frequency filters to highlight the presence of the carriers at the device facet. Corresponding theoretical current density and carrier density profiles were used to validate the measured profiles and to quantify the effective lateral spreading of the carriers resulting from the combined effects of current spreading and carrier diffusion, [5]. An effective diffusion length $L_D = 2.4 \ \mu m$ was obtained for the devices of interest here. Therefore, with an inter-element separation $S = 30 \ \mu m$, corresponding to $S - W_T \sim 4L_D$ separation between the ridges of the individual elements at the facet, the individual elements in the array are considered to be independent (uncoupled).

All devices were bonded p-side down on temperature stabilized copper mounts ($T = 20°C$). However, thermal management was not optimized. Therefore, to reduce the risk of

breakage, the devices were tested predominantly using pulsed current with 0.1% duty cycle (200-Hz repetition rate, 5-μs pulse duration). In this context, the continuous-wave (CW) results presented in the next Section are only preliminary at this stage, but they seem to confirm the trends observed under pulsed operation. Indeed, thermal-lensing is expected to play an important role under CW operation since the effective refractive index steps involved in such devices are small. Therefore, further design refinements will be necessary under those conditions to achieve diffraction-limited operation.

III. DEVICE OPERATIONAL CHARACTERISTICS

A. Electrical and Optical Characterization

Representative power-current (P–I) and voltage-current (V–I) characteristics measured from the uncoated arrays and corresponding wall-plug (W-P) efficiency curves (per pulse) are compared in Fig. 2. The P–I characteristics measured from PBTLAs and SLAs are compared in detail. The P–I characteristics of LBTLAs are very similar to those of corresponding PBTLAs (inset of Fig. 2). The threshold current densities for all devices are comparable, $J_{th} \sim 0.2 \ kAcm^{-2}$. The voltage across the devices changes only slightly with the inter-element spacing S, and with the device geometry (typical series resistance 0.42Ω). However, the slope efficiency and, as a consequence, the W-P efficiency (per pulse) reduce significantly when $S > W_T$, Fig. 2. Under pulsed operation output powers in excess of 2.8 W/facet and 3.2 W/facet have been measured from 5PBTLA-0s and 5SLA-0s, respectively, and of 2.1 W/facet and 2.5 W/facet from 5PBTLA-10s and 5SLA-10s, respectively, at $22I_{th}$ without catastrophic optical damage (COD), without saturation, and without thermal roll-over.

TABLE I
OPERATIONAL CHARACTERISTICS MEASURED FROM IN-HOUSE FABRICATED 5PBTLA-0S AND 5PBTLA-10S AT $I = 3I_{th}$ AND $I = 7.5I_{th}$ UNDER PULSED (5μS, 200 HZ) AND CW OPERATION

	I_{th} (mA)	Max W-P per pulse (%)	Output Power (W/facet)		θ_x FWHM (deg.)		Brightness ($MWcm^{-2}srad^{-1}$)	
			$I = 3I_{th}$	$I = 7.5I_{th}$	$I = 3I_{th}$	$I = 7.5I_{th}$	$I = 3I_{th}$	$I = 7.5I_{th}$
5PBTLA-0								
Pulsed	160	35	0.3	0.7	0.8	0.8	42	128
CW	160	20	0.2	0.5	3.2	3.0	5	12
5PBTLA-10								
Pulsed	180	31	0.2	0.5	2.8	2.7	5	14
CW	160	9	0.1	0.2	3.2	3.0	2	6

The devices were measured also under CW operation. However because of the lack of proper thermal management the driving current was limited to $I = 1.2A = 7.5\,I_{\rm th}$. Under CW operation, no significant change in threshold current was observed with respect to that measured under pulsed operation, Fig. 2 (for PBTLAs only). On the other hand, the slope and W-P efficiencies were both significantly lower than those measured under pulsed operation, Table I (characteristics of 5PBTLA0s and 5PBTLA10s). From the results presented in Fig. 2, it is noticed that no thermal roll-over has been observed under CW operation over the range of currents investigated. Output powers in excess of 500 mW CW per facet have been measured from 5PBTLA-0s (at $I = 1.2A = 7.5I_{\rm th}$), Fig. 2.

B. Near-Field Intensity Profiles

Although all suitable for high-power operation, the output beam characteristics measured from the above-mentioned devices vary enormously not only with the geometry of the optical cavity, [4], but also, as expected, with the inter-element spacing S. The near-field intensity profiles measured from the laser arrays at and above threshold (pulsed operation) are presented in Fig. 3, clearly showing the presence of the inter-element spacing in arrays with $S > W_T$. The features of the near field are noticeably different when $S = W_T$, indicating different modes of operation of the two types of devices (of all geometries).

C. Far-Field Characteristics

The far-field intensity profiles measured without the use of lenses are presented in Fig. 4 (pulsed operation). The angular resolution of such measurements is 0.05 deg near threshold the far fields measured from all coupled devices $(S = W_T)$ are typically double-lobed indicating that the highest order mode has the highest modal gain, as expected in these conditions. From the simple diffraction theory point of view the two-lobe profile observed at threshold indicates that there is a π-phase-shift between adjacent elements in the array, [10]. The measured lobe separation is 2.8 deg, in agreement with that predicted the CMT, [5], $\Delta\theta = \arcsin((\lambda/S))$. At higher currents the far field becomes single-lobed only in arrays of coupled bow-tie lasers, indicating dominant fundamental mode operation in such devices. The change in mode operation in such devices is due to the combined effects of spatial-filtering (operated by the narrow central stripes) and of hole-burning which changes the gain and refractive index distributions across the device, thereby increasing the fundamental mode gain, [4], [5]. In particular, the best results
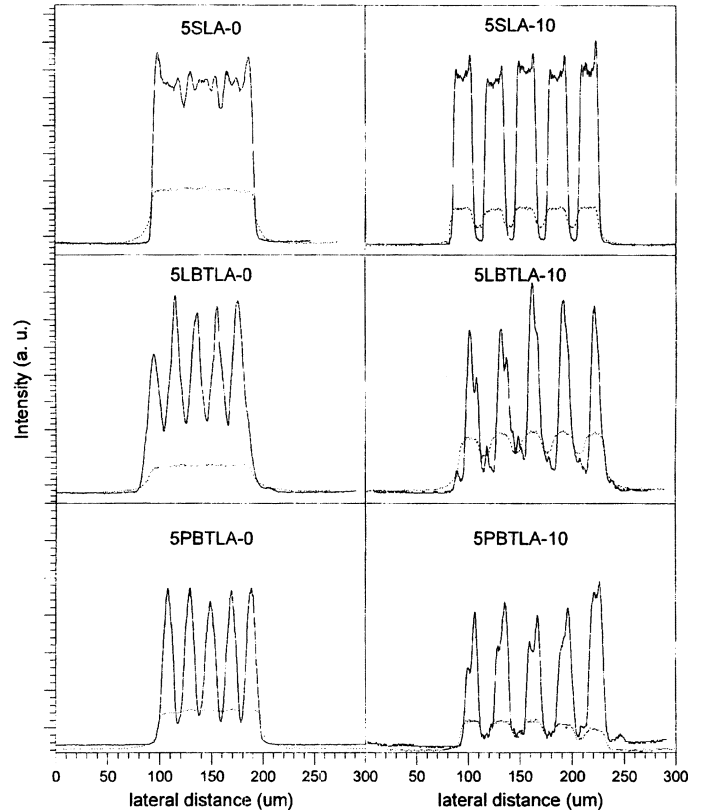

Fig. 3. Near-field intensity profiles measured from 5PBTLA-0s, 5PBTLA-10s, 5LBTLA-0s, 5LBTLA-10s, 5SLA-0s, and 5SLA-10s below (dotted lines) and above (solid lines) threshold, at $I \sim 20$–50 mA and $I = 1$–1.5 A, respectively. (Measurement resolution: 3 μm.)

are obtained from 5PBTLA-0s, where the contribution of the higher order array modes is negligible. This experimental observation gives evidence of the fact that in the arrays of coupled PBTLs, the individual elements operate in phase. Therefore, in this case, the resulting self-consistent optical field profile very closely resembles that of the fundamental mode of an array of strongly coupled stripes (each of width W_T) or, equivalently, that of a wide stripe of width W. In Fig. 4, the experimental far-field profiles are compared with those calculated with the coupled mode theory for the fundamental modes of the arrays of interest. Under pulsed operation PBTLA-0s remain near-diffraction-limited, that is, beam width < 2DL (diffraction-limited) up to $I = 20I_{\rm th} = 3.2$ A, corresponding to (pulsed) output optical powers up to 2.4 W, [4]. At higher
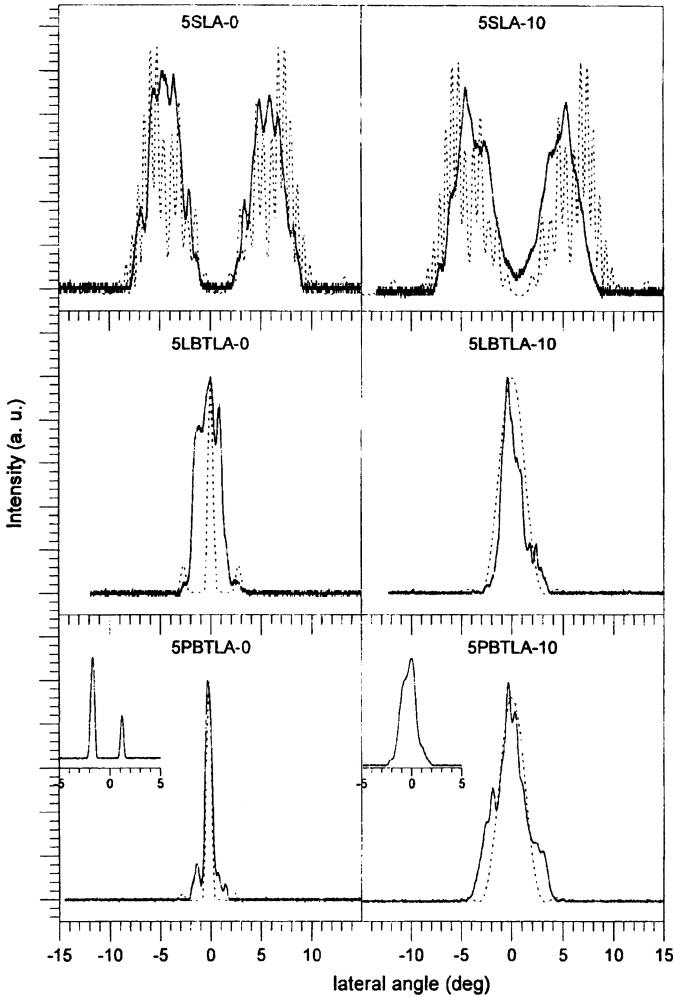
Fig. 4. Comparison of far-field intensity profiles measured (solid lines) from 5PBTLA-0s, 5PBTLA-10s, 5LBTLA-0s, 5LBTLA-10s, 5SLA-0s, and 5SLA-10s, near threshold (insets), and at $I = 20 I_{\text{th}}$ under pulsed operation. (Measurement resolution: 0.05 deg.) Corresponding theoretical profiles (dashed line) obtained with the coupled mode theory are also presented for completeness.

Fig. 5. Far-field intensity profiles measured under CW operation (solid line) at and above threshold ($I = 7.5 I_{\text{th}}$), from (a) 5PBTLA-0s and (b) 5PBTLA-10s. (No lenses were used; angle resolution: 0.05 deg.) Corresponding theoretical profiles (dashed line) obtained with the coupled mode theory are also presented for completeness.

currents (up to the measured $I = 22 I_{\text{th}} = 3.5$ A) the far field broadens to approximately 2DL since higher order array modes begin to significantly contribute, as evidenced by the fact that the lateral peaks in the far-field intensity profile become more pronounced.

For 5SLA-0, the far-field intensity pattern remains double-lobed, indicating that in this case (as expected) the highest order mode has the highest modal gain. In Fig. 4, the experimental profile is compared with that calculated using the coupled mode theory from an array of narrow ($W_T = 1\ \mu$m) stripes to simulate the effect of hole-burning. The good agreement between theory and experiment indicates that in this case hole-burning is not favouring fundamental mode operation (however, it is essential to include hole-burning to account for the observed peaks).

The far fields measured at threshold from uncoupled arrays ($S > W_T$) are always single-lobed except for the SLAs. In 5SLA-10, in fact, multimode operation is manifestly producing a double-lobed far-field pattern, but with nonzero field on axis (significantly different from the case of 5SLA-0s, where the far-field pattern presents an on axis null). The FWHM measured
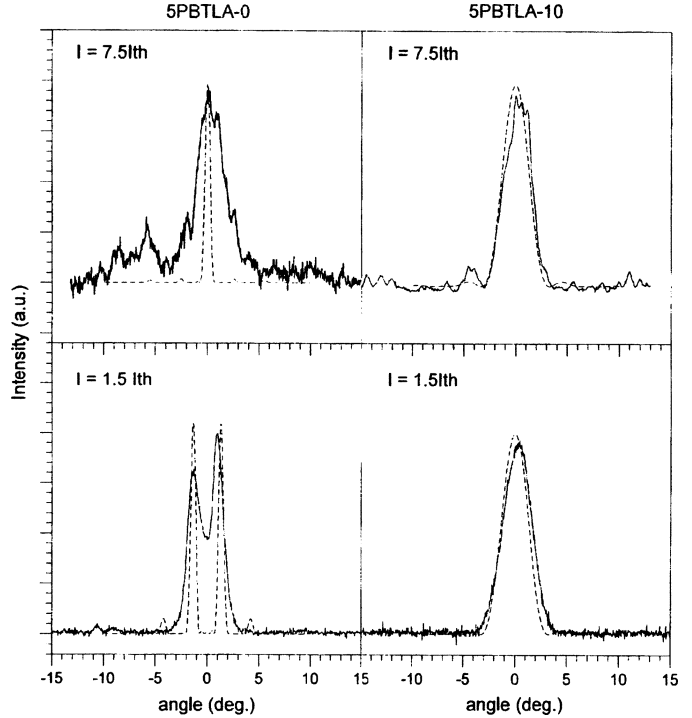
from 5PBTLA-10s and 5LBTLA-10s is independent on the operating current, indicating that the elements in those arrays are operating independently. The measured FWHM of the far field is 2.7 deg, approximately equal to that of an individual element.

The far fields measured under CW operation, Fig. 5 (for PBTLAs only), confirm the trends discussed above. It is noted, however, that the peak separation measured from coupled PBTLA-0s at threshold under CW operation (2.5 deg) is slightly smaller than that measured under pulsed operation, because of the thermal lensing that typically occurs under CW operation. At higher currents the CW far fields measured from coupled arrays are single-lobed, but with FWHM (3 deg) significantly broader than that measured under pulsed operation. This broadening of the far field under CW operation is attributed to the present, inefficient thermal sinking—local heating reduces the available gain, promoting multi-mode operation. Finally, also under CW operation the far-field profiles measured from arrays of uncoupled devices ($S > W_T$) are comparable with those obtained from individual elements substantiating the features discussed above in connection with the measurements taken under pulsed operation.

IV. BRIGHTNESS AND COHERENCE MEASUREMENTS

The measured lateral far-field FWHM and estimated brightness as functions of driving current are presented in Fig. 6 for coupled and un-coupled arrays of all geometries. In addition, the Strehl ratio (SR) was also estimated experimentally by measuring the optical power through slits of aperture corresponding to the diffraction-limit divergence angle, placed at the far-field
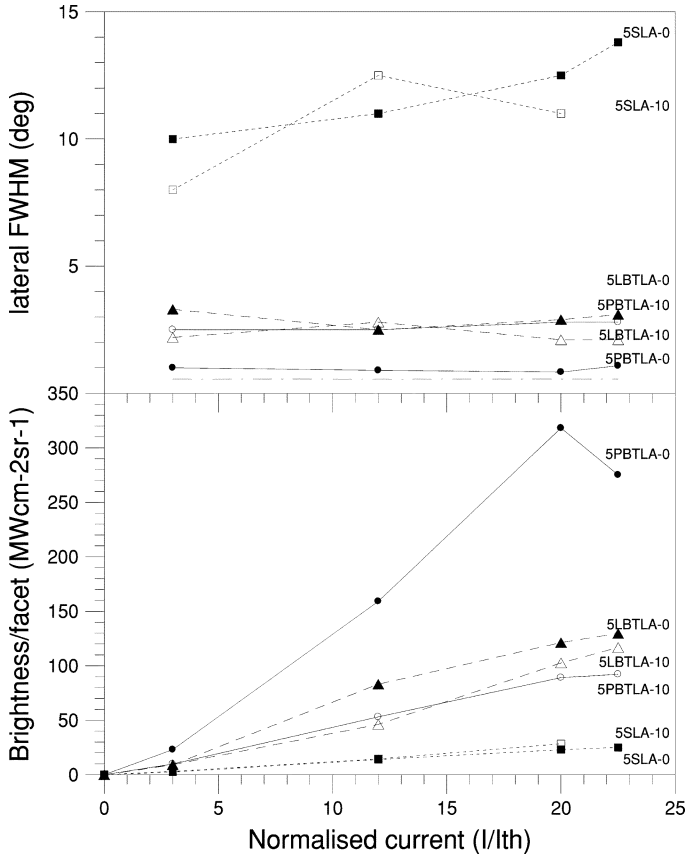
Fig. 6. Brightness (per facet) and lateral far-field intensity FWHM as functions of the injection current normalized with respect to I_{th} for coupled and uncoupled uncoated arrays of different geometry (dash-dotted line represents the diffraction limit estimated for a 100-μm aperture; other lines as indicated).

plane. This parameter gives an indication of the effectiveness of the laser design since diffraction-limited operation can also be achieved in a situation where multiple peaks are present—therefore, in such cases it is essential to ensure that the power in the side lobes is minimal. The diffraction-limit angle, $\theta_d = \arcsin((\lambda/D)) = 0.56$ deg, estimated from a uniformly illuminated 100-μm aperture is also included in the graph as a reference. It is noted that the minimum FWHM (0.83 deg) value was measured from 5PBTLA-0s at $20I_{th}$, corresponding to 1.5 the diffraction-limit. At that operational current, the brightness was highest, reaching 318 MW·cm^{-2}sr^{-1}, Fig. 6. In addition, the FWHM of the far field measured from those arrays is considerably narrower than that measured from an individual PBTL (2.8 deg), [8], indicating that in-phase inter-element coupling (fundamental array mode operation) is effectively taking place. Correspondingly, the peak 70% SR measured from 5PBTLA-0s occurs at $I = 20I_{th}$, decreasing at higher currents because of the far-field broadening. The arrays of linearly tapered lasers did exhibit single mode far field, however in-phase operation was never observed and, therefore, the brightness achieved in this case is modest (130 MW·cm^{-2}sr^{-1}). This is due to the reduced adiabaticity of the linear taper geometry, where the coupling to higher local modes within each taper is more significant than in tapers of parabolic geometry, [5].

For the uncoupled ($S > W_T$) arrays the brightness varies almost linearly with current, as presented in Fig. 6, because

the FWHM is independent of the operating current. The brightness achieved from 5PBTLA-10s and 5LBTLA-10s are comparable ($\sim$100 MW·cm^{-2}sr^{-1}, at $20I_{th}$) but still considerably lower than that achieved from an individual PBTL (137 MW·cm^{-2}sr^{-1} at $I = 20I_{th}$) or from 5PBTLA-0s (318 MW·cm^{-2}sr^{-1} at $I = 20I_{th}$).

On the other hand, the brightness measured from stripe arrays (both coupled and un-coupled) is significantly lower (25 MW·cm^{-2}sr^{-1}) than that measured from the arrays of bow-tie lasers discussed above. This is a direct consequence of the fact that the far fields obtained from such lasers are typically double-lobed, with correspondingly low SR.

Under CW operation the highest brightness achieved from PBTLA-0s is 12 MW·cm^{-2}sr^{-1} at $I = 7.5I_{th}$, which is one order of magnitude lower than that obtained under pulsed operation at the same current (128 MW·cm^{-2}sr^{-1} at $I = 7.5I_{th}$), and 6 MW·cm^{-2}sr^{-1} at $I = 7.5I_{th}$ for 5PBTLA-10s.

Ideally the total power emitted by an array of N identical elements is N times the power emitted from an individual element. If the array is coherently coupled and operates in the fundamental (in-phase) mode, the emitted beam is single-lobed and its lateral divergence at FWHM is $1/N$ times the divergence of an individual emitter. As a consequence, since the total area of emission is N times that of an individual emitter, the brightness of the array is N times the brightness of an individual element [1]. In practice, for the devices of interest in this paper the scaling factors, $N_{(P)}$ and $N_{(\theta)}$, estimated respectively from the measured output power and beam divergence differ from the expected value ($N = 5$). Values for $N_{(P)}$ and $N_{(\theta)}$ are summarized in Table II, together with the (compound) factor $N_{(B)}$ derived for the brightness. From the data presented in Table II, it is seen that the closest approximation to the ideal $N (=5)$ is achieved with 5PBTLA-0s, for which $N_{(P)} = 3.9$ and $N_{(\theta)} = 3.4$ and $N_{(B)} = 2.7$.

To further substantiate the above observations, the degree of coherence, or mutual coherence, [11], between the emitters in 5PBTLA-0s and 5PBTLA-10s was estimated using the two-slit experiment. Using a microscope objective lens (NA = 0.25), the near field of the array was imaged onto 100-μm transmission slits separated by 1-mm spacing to observe optical interference between two specific elements of the array. The interference pattern was imaged onto a charged couple device (CCD) camera. The interference fringes obtained at different currents from the two types of arrays are presented in Fig. 7. To estimate the coherence of the array the modulus of the complex degree of coherence $|\gamma_{mn}|$, also called coherence or mutual coherence, [11], was calculated from the visibility of the fringes

$$|\gamma_{mn}| = \frac{I_{\max} - I_{\min}}{I_{\max} + I_{\min}} \qquad (1)$$

where $I_{\max}$ and $I_{\min}$ are, respectively, the maximum and minimum intensity in the interference intensity pattern obtained from elements m and n in the array. It is noted that in such measurements the path differences are typically smaller than the coherence length (which is of the order of millimeters) and, therefore, the quantity measured is effectively the spatial coherence.

The mutual coherence estimated for adjacent elements in 5PBTLA-0s, Fig. 7, is $\gamma_{mn} = 0.6$ at threshold and $\gamma_{mn} = 0.3$

TABLE II
Pulsed Operational Characteristics Measured at $I = 2I_{th}$ From Individual Elements, Coupled and Uncoupled Arrays; N_P, N_θ, and N_B Are the Scaling Factors Obtained for Optical Power Output, Far Field FWHM, and Brightness (B)

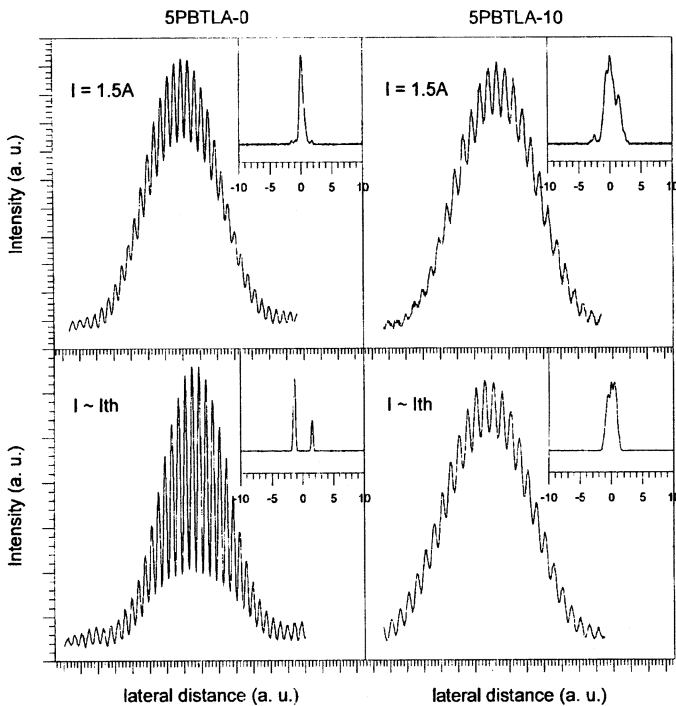|	I_{th} (mA)	η_e (W/A)	Output Power at $20I_{th}$ (W/facet)	N_P	θ_x FWHM at $20I_{th}$ (deg.)	N_θ	B at $20I_{th}$ (MWcm^{-2}srad^{-1})	N_B
PBTL	40	0.7	0.6	1	2.8	1	135	1
5PBTLA-0	160	0.8	2.5	3.9	0.8	3.4	318	2.3
5PBTLA-10	180	0.6	2.0	3.1	2.7	1	79	0.6
LBTL	55	0.6	0.6	1	2.9	1	107	1
5LBTLA-0	160	0.8	2.1	3.7	2.8	1.3	89	0.8
5LBTLA-10	180	0.6	2.0	3.5	2.9	1	72	0.7
SL	60	0.8	0.7	1	3.2	1	62	1
5SLA-0	200	0.8	2.8	4	12.5	0.3	25	0.4
5SLA-10	220	0.7	2.7	3.9	12.2	0.3	15	0.2

Fig. 7. Interference fringes obtained from adjacent elements in 5PBTLA-0s and 5PBTLA-10s obtained under pulsed operation near threshold, $I \sim I_{th}$, and at $I = 1.5A \sim 9.5I_{th}$; corresponding far-field intensity profiles measured at those currents are presented in the insets.

above threshold, with $n = m + 1$, for all m. In addition, it is observed that below threshold the peak of the diffraction envelope coincides with a fringe minimum indicating out-of-phase coupling (array operating in the highest order mode). On the other hand, above threshold the peak of the diffraction envelope coincides with a fringe maximum, a reflection of the fact that the fundamental array mode is dominant. However, higher order modes also contribute to the lasing field which can explain the reduction of the mutual coherence observed at higher currents.

The degree of coherence between elements in uncoupled $(S > W_T)$ arrays is negligible ($\gamma_{mn} = 0.1$ for any n and m, Fig. 7), as expected for arrays of incoherently coupled elements, irrespective of driving current, of element-pair position in the array.

V. CONCLUSION

Experimental and theoretical results have been presented to show that in-phase locking (fundamental array mode operation) has been achieved with arrays of PBTLs with simple and inexpensive device fabrication. The novelty of the index-guided PBTLAs described in this paper is that array mode selection is operated by the combined effects of tapered geometry, mode-filtering and hole-burning. The highest brightness obtained from phase-coherent arrays of PBTLs was 318 MW·cm^{-2}sr^{-1} at $20I_{th}$, where the far-field FWHM was at the minimum measured value of 0.83 deg, equivalent to less than 1.5 times the diffraction-limit (measured without lenses). The above results were discussed in the context of lateral phase coherence. Evidence of coherent coupling was further confirmed with results from double-slit interference experiments, leading to the conclusion that phase-coherence (fundamental array mode operation) was observed here only in (index-guided) arrays of parabolic bow-laser arrays.

REFERENCES

[1] D. Botez and D. R. Scifres, *Diode Laser Arrays*. Cambridge, U.K.: Cambridge Univ. Press, 1994.
[2] W. Streifer, A. Hardy, R. D. Burnham, and R. D. Scifres, "Single-lobe phased-array diode lasers," *Electron. Lett.*, vol. 21, no. 3, pp. 118–120, Mar. 1985.
[3] H. Yang, L. J. Mawst, M. Nesnidal, J. Lopez, A. Bhattacharya, and D. Botez, "10 W near-diffraction-limited peak pulsed power from Al-free, 0.98 μm-emitting phase-locked antiguided arrays," *Electron. Lett.*, vol. 33, no. 2, pp. 136–137, Jan. 1997.
[4] F. Causa and D. Masanotti, "High-brightness index-guided parabolic bow-tie laser arrays," *IEEE Photon. Technol. Lett.*, vol. 16, no. 9, pp. 2000–2002, Sep. 2004.
[5] J. K. Butler, D. E. Ackley, and D. Botez, "Coupled-mode analysis of phase-locked injection laser arrays," *Appl. Phys. Lett.*, vol. 44, no. 3, pp. 293–295, 1984.
[6] D. Masanotti and F. Causa, "Optical guiding properties of high-brightness parabolic bow-tie laser arrays," *IEEE J. Quantum Electron.*, vol. 41, no. 7, pp. 909–916, Jul. 2005.

[7] H. Yang, L. J. Mawst, and D. Botez, "1.6 W continuous-wave coherent power from large-index-step ($Dn = 0.1$) near-resonant, antiguided diode laser arrays," *Appl. Phys. Lett.*, vol. 76, no. 10, pp. 1219–1221, Mar. 2000.

[8] D. Masanotti, F. Causa, and J. Sarma, "High brightness, index-guided parabolic bow-tie laser diodes," *Proc. IEE Optoelectron.*, vol. 151, no. 2, pp. 123–128, Apr. 2004.

[9] A. F. Milton and W. K. Burns, "Mode coupling in optical waveguide horns," *IEEE J. Quantum Electron.*, vol. QE-13, pp. 828–835, Oct. 1977.

[10] D. R. Scifres, W. Streifer, and R. D. Burnham, "Experimental and analytical studies of coupled multiple stripe diode lasers," *IEEE J. Quantum Electron.*, vol. QE-15, no. 9, pp. 917–922, 1979.

[11] G. A. Evans and J. M. Hammer, Eds., "Surface emitting semiconductor lasers and arrays," in *Quantum Electronics, Principles and Applications*. San Diego, CA: Academic, 1993.

F. Causa (M'98) received the Laurea degree in physics from the University of Milan, Milan, Italy, in 1993 and the Ph.D. degree from the University of Bath, Bath, U.K., in 1998.

She joined the Department of Electronic and Electrical Engineering, University of Bath, as a Lecturer in 1999. Her research experience includes the modeling, design, and characterization of semiconductor optical devices. In 2001, she was seconded to Bookham Technology, Caswell, U.K., for a period of six months via an Industrial Secondment Scheme funded by the Royal Academy of Engineering. Recently, she has collaborated with scientists in Tata Institute of Fundamental Research, Mumbai, India (British Council sponsored India-U.K. Young Scientist Networking Scheme, 2003) and in Max Born Institute fur Nichtlineare Optik und Kurzzeitspectroscopie, Berlin, Germany (VI European Framework Programme Laser-Lab Europe for the characterization of advanced high brightness semiconductor sources, 2005). She is currently involved in the application of high-brightness parabolic laser arrays in medicine with a British-Italian partnership program for young researchers, sponsored by the British Council. Her present research interests include the development of high-power lasers with high-brightness high-power super-luminescent diodes and modeling of nonlinear optical media.

D. Masanotti received the Laurea degree in electronic engineering from the University of Ancona, Ancona, Italy, in 1999 and the Ph.D. degree on the development of semiconductor lasers for high-power high brightness from the University of Bath, Bath, U.K., in 2005.

In 1999, she joined the Department of Electronic and Electrical Engineering, University of Bath, Bath, U.K., as a research officer for a project on the development of Fabry–Perot Laser Diodes for use in chaotic optical encryption experiments. She is currently at the University of Bath, where she is working on the development and modeling of a neurons/silicon-based electronic circuit interface for noninvasive recording of neural activity.